ELSEVIER

Journal of Applied Geophysics 42 (1999) 333–346

JOURNAL OF APPLIED GEOPHYSICS

www.elsevier.nl/locate/jappgeo

Estimation of kinematic wavefront characteristics and their use for multiple attenuation

Jörg Zaske *, Shemer Keydar, Evgeny Landa

The Geophysical Institute of Israel, P.O. Box 182, Lod 71100, Israel

Abstract

Kinematic wavefront characteristics of primary reflected waves can be used to predict and attenuate surface-, as well as interbed multiples. In order to estimate kinematic wavefront characteristics directly from unstacked data the common-shot-point homeomorphic-imaging (CSP HI) method can be applied. This macro-model-independent method is based on a new local moveout correction that depends on two wavefront parameters: the emergence angle and the radius of wavefront curvature of a reflected primary wavefront. These parameters can be estimated by optimizing the semblance correlation measure, calculated in the common-shot-gather along the travel time curve defined by the new moveout correction. In the case of local maxima in the semblance functional, an automatic maximization procedure might lead to a wrong estimation of these parameters. In order to avoid such a situation we propose an interactive, horizon-based implementation of the CSP HI method, which allows manual picking of the optimal wavefront parameters along the seismic line. Afterwards, we use the estimated emergence angles for the prediction and attenuation of multiples, based on the simple but powerful idea that any multiple event can be represented as a combination of primaries. A synthetic example shows the viability of the parameter estimation, prediction and attenuation procedure.

Keywords: Wavefront parameters; Multiple attenuation; Homeomorphic imaging

1. Introduction

Kinematic wavefront characteristics of seismic reflections, such as the arrival time and emergence angle, play a key role in many applications (e.g., ray-based migration, τ–p analysis, etc.). Recently, Keydar et al. (1998) proposed to use the emergence angle of primary reflected wavefronts for the prediction of multiples. Several algorithms have been suggested for the derivation of the emergence angle of a given reflected wavefront at a certain receiver position (Shultz and Clearbout, 1978; Biondi, 1992). They usually involve numerical differentiation procedures, which are known to be highly sensitive to uncertainties in the travel times, or slant–stack procedures, which assume a locally linear travel time approximation. An alternative approach to estimate the emergence angle was proposed by Keydar et al. (1996), who directly estimated the emergence angle from unstacked data. This is done by means of the common-shot-point homeomorphic-imaging (CSP HI) method (Gelchinsky, 1989). A crucial advantage of this approach is that it is macro-model-independent: it only requires information about the near surface velocity.

* Corresponding author. Fax: +972-3-5502-925; e-mail: jzaske@iprg.energy.gov.il

0926-9851/99/$ - see front matter
PII: S0926-9851(99)00044-0

Using the estimated kinematic wavefront characteristics of primary reflections, Keydar et al. (1998) introduced a target-oriented approach to predict multiple arrival times, which is valid for surface-, as well as for interbed multiples. The target-oriented strategy is especially helpful in cases, where the question arises whether a particular event is affected by a multiple. The key point in this procedure is the simple but powerful idea that any multiple, no matter how complicated its ray code, can be represented as a logical combination of primaries. Using this prediction method, Landa et al. (1999b) constructed a multiple model in order to attenuate multiples in the parabolic τ–p domain. Jakubowicz (1998) used a similar idea in a wave equation based approach to construct a multiple model from primary events and applied least squares filtering for the subtraction.

We propose a new, interactive and user-friendly procedure for the estimation of kinematic wavefront characteristics along the picked zero-offset travel times of a specified horizon. This procedure is essentially an application of the CSP HI method for the special case of a horizon-based parameter estimation. It consists of manual picking of optimal emergence angles along the horizon in a semblance panel. Manual picking based on a priori information has the important advantage that it can resolve ambiguity problems in cases, where automatic procedures fail. Following the work of Keydar et al. (1998) and Landa et al. (1999a; b), we use the estimated wavefront parameters for the prediction and attenuation of multiple reflections. A representative example is used to illustrate the parameter estimation, prediction and attenuation method.

2. Multiple prediction and attenuation procedure

Let us consider the interbed multiple in Fig. 1. The multiple raypath A_sBCDA_r can be considered as the combination of the primary raypaths A_sBA_m and A_nDA_r minus the primary raypath A_nCA_m. This means that the travel time of the interbed multiple in Fig. 1 can be described using the travel times of the primaries reflected from the multiple generating interfaces i, j and k:

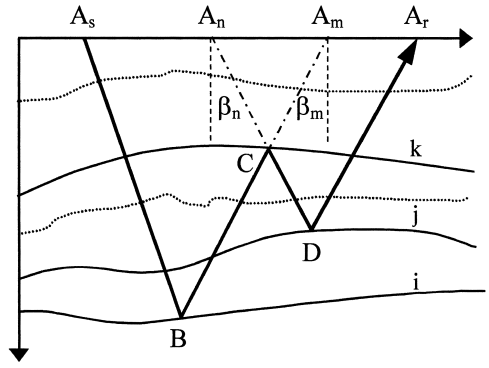

Fig. 1. Ray scheme of an interbed multiple event (A_sBCDA_r). The arrival time of this multiple is a simple combination of three primary arrival times, namely A_sBA_m, A_nCA_m and A_nDA_r. The emergence angle β_m is identical for the rays A_sBA_m and A_nCA_m, and the emergence angle β_n is identical for the rays A_rDA_n and A_mCA_n.

$$T_{sr}^{ikj} = T_{sm}^{i} + T_{nr}^{j} - T_{nm}^{k} \quad (1)$$

where T_{sr}^{ikj} is the travel time of the multiple A_sBCDA_r via reflectors i, k and j, T_{sm}^{i} is the travel time of the primary A_sBA_m reflected from interface i, T_{nr}^{j} is the travel time of the primary A_nDA_r reflected from interface j and T_{nm}^{k} is the travel time of the primary A_nCA_m reflected from interface k. The upper index denotes the number of the reflector, the first lower index denotes the location of the shot and the second the location of the receiver.

In order to predict the travel time of a specified multiple using Eq. (1), we need to know the traces containing the multiple generating primaries for each source–receiver pair A_s and A_r (Fig. 1). We find these traces by using the multiple prediction method based on the HI technique. This method uses ‘multiple conditions’, which claim that the emergence angles of the involved primaries are identical. This is

explained in Fig. 1: The emergence angle of the wavefront of the primary reflection A_sBA_m from reflector *i* is identical to the emergence angle of the primary reflection A_nCA_m from reflector *k*. Similarly, the emergence angle of the primary reflection A_rDA_n from reflector *j* is identical to the emergence angle of the primary reflection A_mCA_n from reflector *k*. In summary:

$$\beta_{sm}^{i} = \beta_{nm}^{k};\ \beta_{rn}^{j} = \beta_{mn}^{k} \qquad (2)$$

where β is the emergence angle of the wavefront, and the lower and upper indices are chosen according to the notation in Eq. (1). These conditions can be used to find the multiple generating traces of the involved primaries. First, we need to estimate the emergence angles of the primary reflections, which generate a specified multiple for all source–receiver positions in every shot-gather along a seismic line. Second, we find those traces, which satisfy the multiple conditions in Eq. (2). The crucial step is the estimation of the emergence angle of a given primary reflection for each shot at every receiver position.

We estimate the angle of emergence directly from unstacked data using the CSP HI technique. This method is described in detail in Keydar et al. (1996; 1998). The basis of the CSP HI method is a new moveout correction that depends on two wavefront parameters, the emergence angle and the radius of wavefront curvature of a primary reflection, as well as on the near surface velocity. The derivation of this moveout formula with respect to the normal ray is illustrated in Fig. 2: a reflection wavefront Σ emerges at the zero-offset location A_0 at an angle β_0. This wavefront can be approximated in the vicinity of A_0 by a fictitious circular wavefront with radius of curvature R_0 and the same emergence angle β_0. From simple geometrical considerations and the use of the cosine-theorem, it follows that the moveout correction ($\Delta\tau_k$) at a point A_k can be expressed as

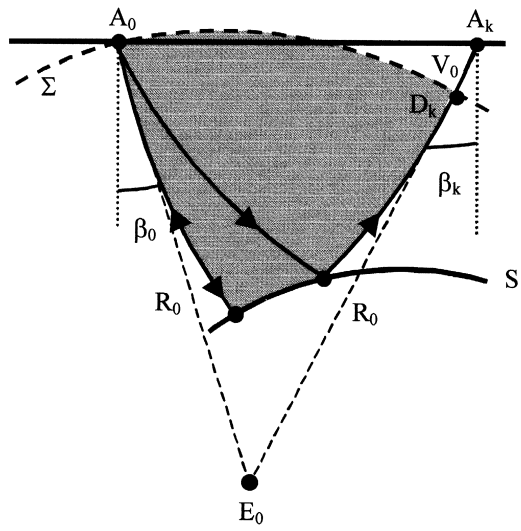

Fig. 2. Ray diagram illustrating the estimation of the emergence angle and the radius of wavefront curvature for the normal ray. Two rays are emitted from the source point A_0. The wavefront Σ emerges at A_0 with an angle β_0 and at A_k with an angle β_k. The radius of wavefront curvature of this spherical wavefront is R_0. The moveout correction $\Delta\tau_k$ and the offset-dependent emergence angle β_k are functions of β_0, R_0, Δx, and the near surface velocity V_0.

a function of the angle of emergence and the radius of wavefront curvature of the normal ray at point A_0:

$$\Delta\tau_k = \frac{\sqrt{R_0^2 + 2R_0\Delta x \sin\beta_0 + \Delta x^2} - R_0}{V_0} \qquad (3)$$

where β_0 and R_0 denote the emergence angle and the radius of wavefront curvature of the reflected shot wave at A_0, V_0 the near surface velocity and Δx the offset between the source at A_0 and the receiver at A_k.

In order to find the unknown wavefront parameters R_0 and β_0 a special semblance maximization procedure, similar to conventional velocity analysis, has been developed. It is applied in the common-shot-gather along the travel time curve defined by the moveout correction in Eq. (3). The near surface velocity should either be known or can be one of the search parameters. Semblance maximization is carried out using an optimization algorithm. We perform the search around the zero-offset time of a specified pri-

mary reflection (interpreted from a stacked section).

Once the optimal emergence angle and the radius of wavefront curvature corresponding to the normal ray, β_0 and R_0, have been estimated for all shot positions, we obtain the angle of emergence β_k for an arbitrary trace k with offset Δx using the following expression, which follows again from the spherical wavefront assumption and simple geometrical considerations (Fig. 2):

$$\sin \beta_k = \frac{\Delta x + R_0 \sin \beta_0}{\sqrt{R_0^2 + 2 R_0 \Delta x \sin \beta_0 + \Delta x^2}}. \qquad (4)$$

Using these emergence angles, we find the traces containing the multiple generating primaries: For each shot–receiver position in every common-shot-gather, we search for intermediate points satisfying the specified multiple conditions (e.g., defining points A_n and A_m in Fig. 1). The travel times of the primaries, which generate multiples on the trace located at these intermediate points can be used in Eq. (1) to calculate the multiple arrival times, assuming that the primary travel times are known. In this way, we can predict multiples of any type and order.

From the predicted multiple travel times a multiple model can be constructed, followed by multiple subtraction. Similar to Zhou and Greenhalgh (1996) and Landa et al. (1999a; b), we choose the parabolic τ–p domain in order to do the filtering. In the parabolic τ–p domain the separation of primaries is better than in the x–t, f–k or τ–p domain (e.g., Hampson, 1986; Zhou and Greenhalgh, 1994). The maximum energy of an event in the x–t domain is compressed to the vicinity of a point in the τ–p domain. This point can be predicted by a parabolic approximation of the multiple travel time curve, which was predicted in the x–t domain using the described prediction method. After the multiple is predicted in the τ–p domain it can be filtered out by simple muting of the predicted area followed by an inverse τ–p transformation. Alternatively, all but the predicted multiple area in the τ–p domain can be muted. This leads to the multiple model in the parabolic τ–p domain. In order to get the multiple model in the x–t domain an inverse τ–p transformation is performed, followed by filtering in the x–t domain. The latter way is preferable in the sense that primary data, which are not interfering with multiples, are not damaged by forward and inverse τ–p transformations (Kelamis et al., 1990). However, if the predicted undesired multiple and a desired primary have the same zero-offset time, some differential moveout between them is needed in order not to damage the primary.

The main benefit of the proposed method is that no knowledge of the subsurface model or the source wavelet is needed, and there is no special requirement that the input data contain near-offset or zero-offset data.

3. Implementation

Our implementation of the multiple prediction and attenuation method follows the ideas of Section 2. After the multiple generating primaries have been identified and their zero-offset travel times have been picked in a stacked section, the wavefront parameters for the corresponding normal rays are estimated using the CSP HI method. The fact that our search of the unknown parameters is organized along specified horizons allows us to perform a convenient, interactive procedure similar to horizon-velocity analysis (HVA). The difference of our approach is that we are, in fact, searching for two unknown parameters (β_0 and R_0) instead of only one (V_{stack}) in the case of HVA.

3.1. Implementation of the parameter estimation procedure

The implementation of our parameter estimation procedure is based on the correlation of the signal in the observed seismic traces. We estimate the two unknown parameters by maximizing the correlation measure (e.g., semblance), calculated in the common-shot-gather along the

travel time curve defined by the moveout correction in Eq. (3).

For a given emergence angle (β_0) of the normal ray at a specified shot position the optimal radius of the wavefront curvature (R_0) is found automatically by applying a local one-parameter optimization method, which maximizes the semblance correlation measure. This

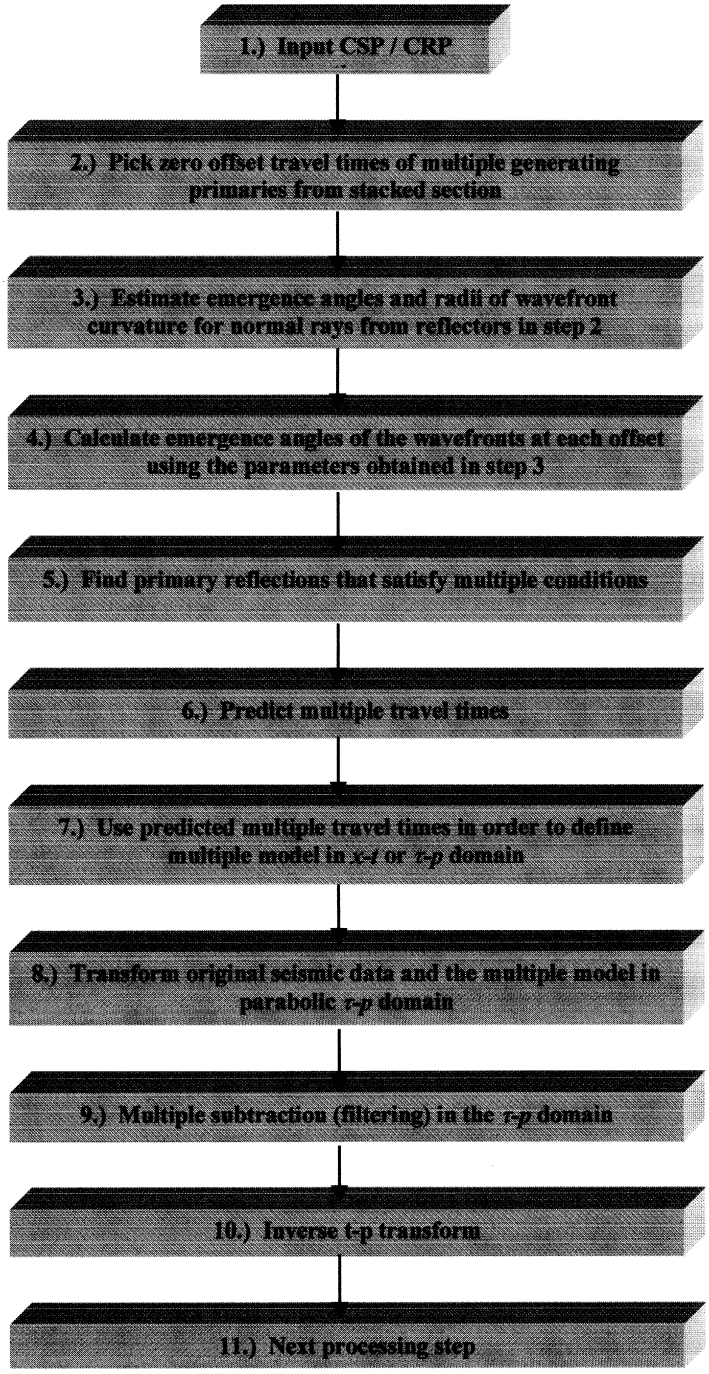

Fig. 3. Flow chart of the multiple prediction and attenuation method.

step is repeated for all possible emergence angles and usually optimal parameters are chosen corresponding to the semblance maximum. Such an approach leads to correct wavefront parameters if the search is done for instance for a relatively strong primary reflection. A basic problem is that automatic procedures optimally stack useful signal as well as noise, especially spatially correlated noise. In addition, the interference between different waves can lead to problems in the correct estimation of the unknown parameters. In such cases, the correlation measure as a function of search parameters might not be unimodal, thus requiring a global optimization strategy. Nevertheless, even the global maximum might be related to interfering events or noise rather than to the signal. For instance, strong multiple reflections may show higher correlation values than weak primary events. In the interactive velocity analysis such an ambiguity is resolved manually by picking the correct maxima on the basis of a priori velocity information.

We address such problematic situations in the case of the horizon-based wavefront characteristics estimation and suggest an interactive procedure. This procedure consists of picking the optimal parameter combination between the emergence angle β_0 and the radius of wavefront curvature of the normal ray R_0, along a specified horizon and is explained in the following.

Using the search procedure described above, the semblance as a function of angle and shot position is defined for all possible angles, when the radius (R_0) for each angle is chosen corresponding to the maximum semblance of the one-parameter search. The results of such a calculation can be displayed in a semblance panel, where the horizontal axis denotes the shot position and the vertical axis the emergence angle (Fig. 5a). In such a semblance panel the optimal emergence angles as a function of shot position can be picked similar to the stacking velocity (V_{stack}) in HVA. As mentioned above an optimal radius R_0 is associated with each picked angle in the semblance plot (Fig. 5b). This gives additional information for the interpreter to decide if the 'pick' was reasonable. As usual, the smoothness of parameters as well as a priori information are leading criteria in our interactive procedure.

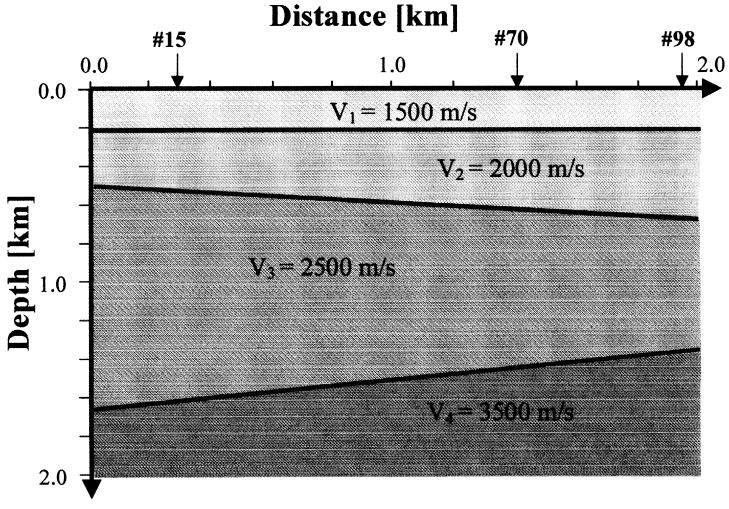

Fig. 4. A three-layer model with dipping interfaces. According to this model 100 common-shot-gathers have been calculated using finite-difference modeling. The receiver spacing and offset increment is 20 m. Each shot-gather consists of 50 traces. The sampling rate is 4 ms. The arrows denote the location of three shot-gathers (#15, #70 and #98), which are displayed in Fig. 9.

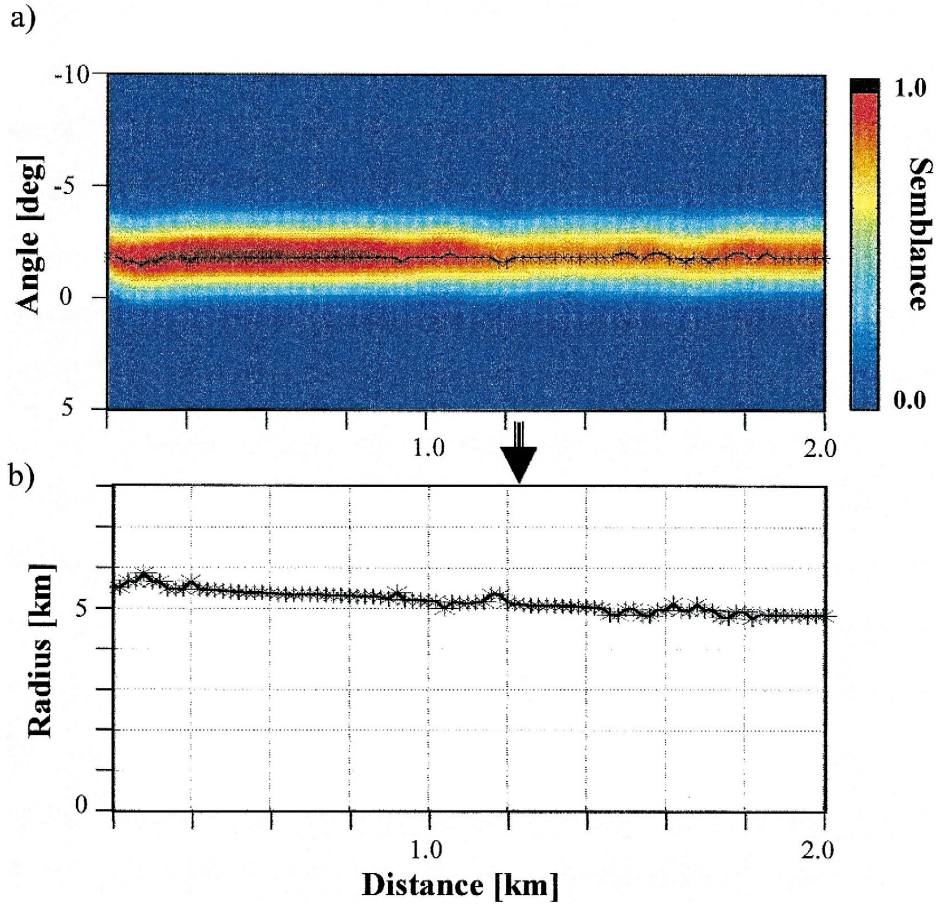

Fig. 5. Illustration of the interactive horizon-based parameter estimation along the picked zero-offset times of the third multiple generating reflector in Fig. 4. (a) Semblance panel as function of shot-position and emergence angle β_0 of the normal ray. Each semblance value is calculated automatically and belongs to a combination between the two parameters, angle β_0 and radius R_0. Picking based on a priori information can resolve ambiguity problems in case of undesired semblance maxima (see text). Each picked angle in (a) belongs to a certain radius, which is shown in (b). In this simple case automatic picking according to the maximum semblance value has been chosen in (a), which gives the corresponding radii in (b).

3.2. Implementation of the prediction and attenuation procedure

In the next step we use these results for the normal rays in order to calculate the emergence angles at different offsets in Eq. (4). Using the offset-dependent emergence angles, we can define the locations of the intermediate points which satisfy the multiple conditions (e.g., A_n and A_m in Fig. 1). This can be done by scanning all possible locations for those traces, which satisfy the specified multiple conditions. If these traces are selected, the travel time of the multiple can finally be predicted using the involved primary travel times in Eq. (1). The arrival time of a primary reflection is calculated using Eq. (2) and the zero-offset arrival time. For the interbed multiple in Fig. 1 the following expression can be obtained:

$$T_{\mathrm{sr}}^{ikj} = T_{\mathrm{sm}}^{i} + T_{\mathrm{nr}}^{j} - T_{\mathrm{nm}}^{k} = T_{\mathrm{s0}}^{i} + \Delta\tau_{\mathrm{sm}}^{i} + T_{\mathrm{n0}}^{j} + \Delta\tau_{\mathrm{nr}}^{j} - T_{\mathrm{n0}}^{k} - \Delta\tau_{\mathrm{nm}}^{k} \quad (5)$$

where T_{s0}^{i}, T_{m0}^{j} and T_{n0}^{k} are the zero-offset times at points A_s, A_m, A_n for the reflectors i, k and j. $\Delta\tau_{sm}^{i}$ is the time correction for shot A_s and receiver A_m for reflector i; $\Delta\tau_{nm}^{k}$ is the time correction for shot A_n and receiver A_m for reflector k; $\Delta\tau_{nr}^{j}$ is the time correction for shot A_n and receiver A_r for reflector j.

In this work we consider the wavefield of the original data set within time windows around the predicted multiple travel times as multiple model, which is used for multiple attenuation. The complete prediction and attenuation method is summarized in a flow-chart (Fig. 3).

4. Synthetic example

We use a three-layer model with dipping interfaces to demonstrate our parameter estimation, as well as the multiple prediction and

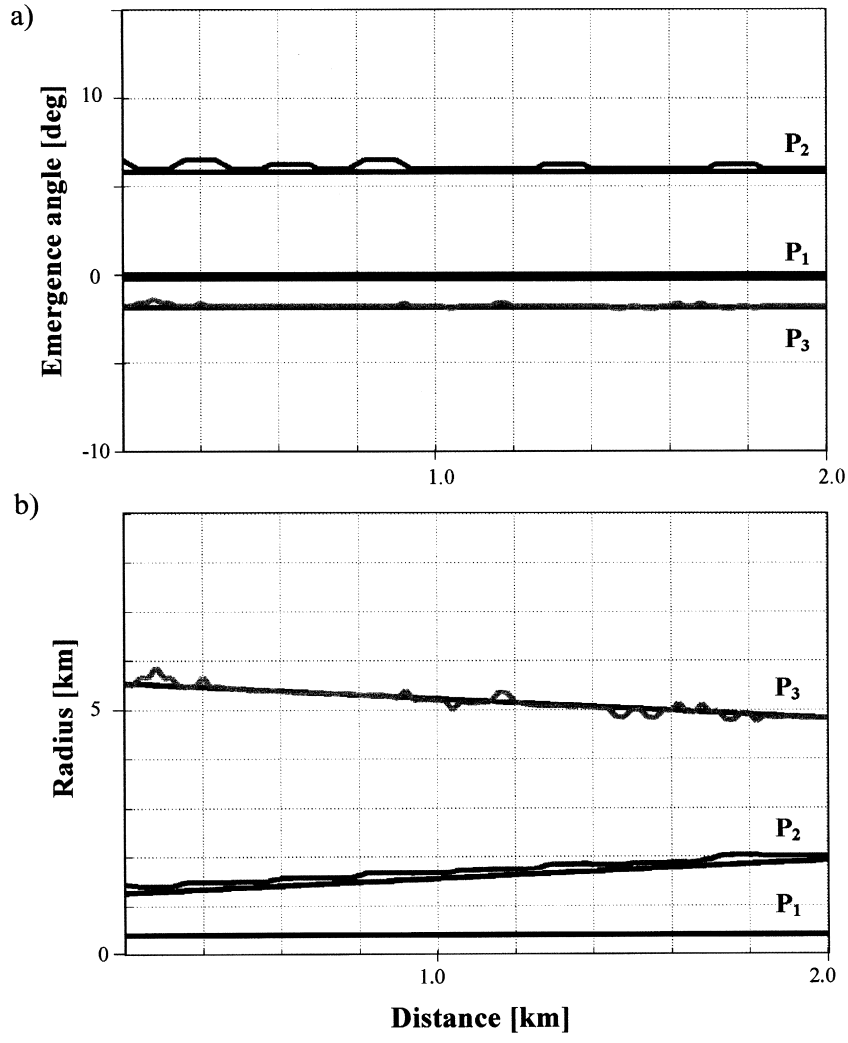

Fig. 6. Results of horizon-based parameter estimation for all three reflectors (Fig. 4), together with the analytical results. (a) Estimated (gray scale) and analytical (black) angles of emergence (β_0) for the primary reflections P_1, P_2 and P_3 from the first, second and third interface (b) estimated (gray scale) and analytical (black) radii of wavefront curvature (R_0).

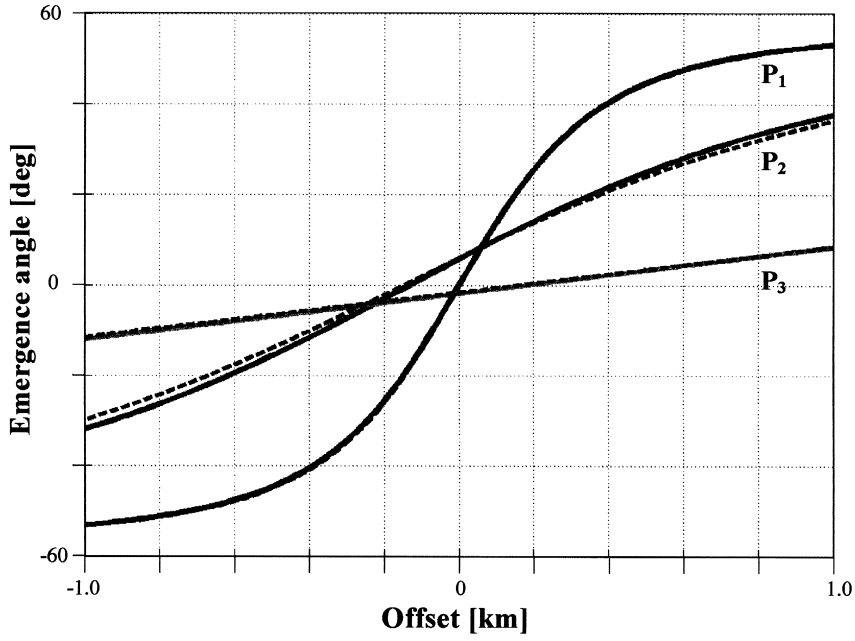

Fig. 7. Offset-dependent emergence angles of the primary wavefronts in one common-shot-gather. The angles have been calculated using the estimated parameters R_0 and β_0 of the normal ray for extrapolation in Eq. (4). The analytical (black) and the estimated (gray scale) results for the primaries P_1, P_2 and P_3 essentially coincide.

attenuation method (Fig. 4). According to this model 100 shot-gathers have been calculated using FD modeling. The receiver-spacing and shot increment is 20 m. Each common-shot-gather consists of 50 receivers. The sampling rate is 4 ms. Due to FD modeling artifacts the data include a high level of correlated noise.

In the first step we estimate the emergence angles of the wavefronts and radii of wavefront curvature for the normal rays from the three interfaces. This is done by applying the described interactive procedure for the parameter estimation along the picked zero-offset travel times of the multiple generating interfaces. It

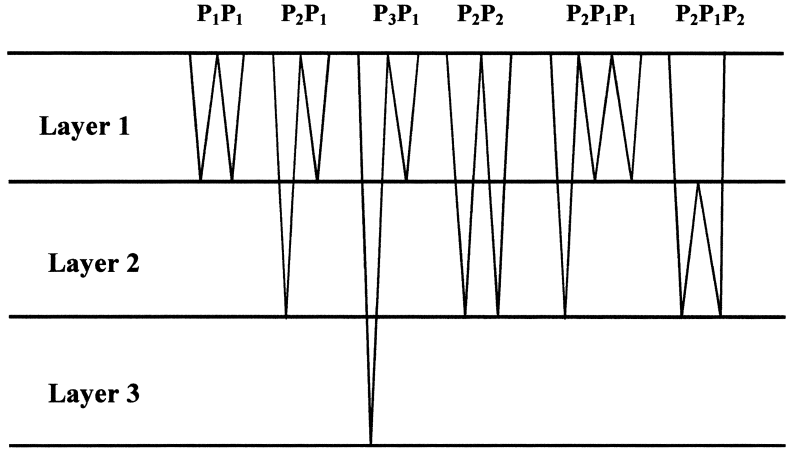

Fig. 8. Ray scheme of six multiple events for which the prediction and attenuation has been done.

consists of displaying the semblance correlation measure as a function of shot position and emergence angle of the normal ray, and picking of the optimal emergence angles as a function of shot position. This situation is shown in Fig. 5a. Each semblance value in this panel belongs to a certain combination of emergence angle and radius of wavefront curvature. This means that each picked emergence angle in this semblance panel has an associated radius of wavefront curvature, which is shown in Fig. 5b.

The picking can be done in an automatic or manual manner. The smoothness of parameters as well as a priori information are leading criteria for the picking. The advantage of manual picking in a semblance panel like in Fig. 5a is that it can resolve ambiguity problems in cases, where the absolute maximum for a certain shot-position is not the desired one and belongs, e.g., to strong coherent noise, which would give a higher semblance maximum than a desired weak primary. In the simple case shown in Fig. 5, automatic picking according to semblance maxima was chosen (black line). The radii, corresponding to these picks are shown in Fig. 5b.

The results of such a parameter estimation procedure for all three multiple generating interfaces in the used model are shown together with the analytical results in Fig. 6. The differences are mainly due to the discretization interval of the scanned angles used for the search and due to step-like, instead of smooth interfaces used for FD modeling. The step-like discretization of dipping reflectors may lead to step-like variations in wavefront parameters. This effect can

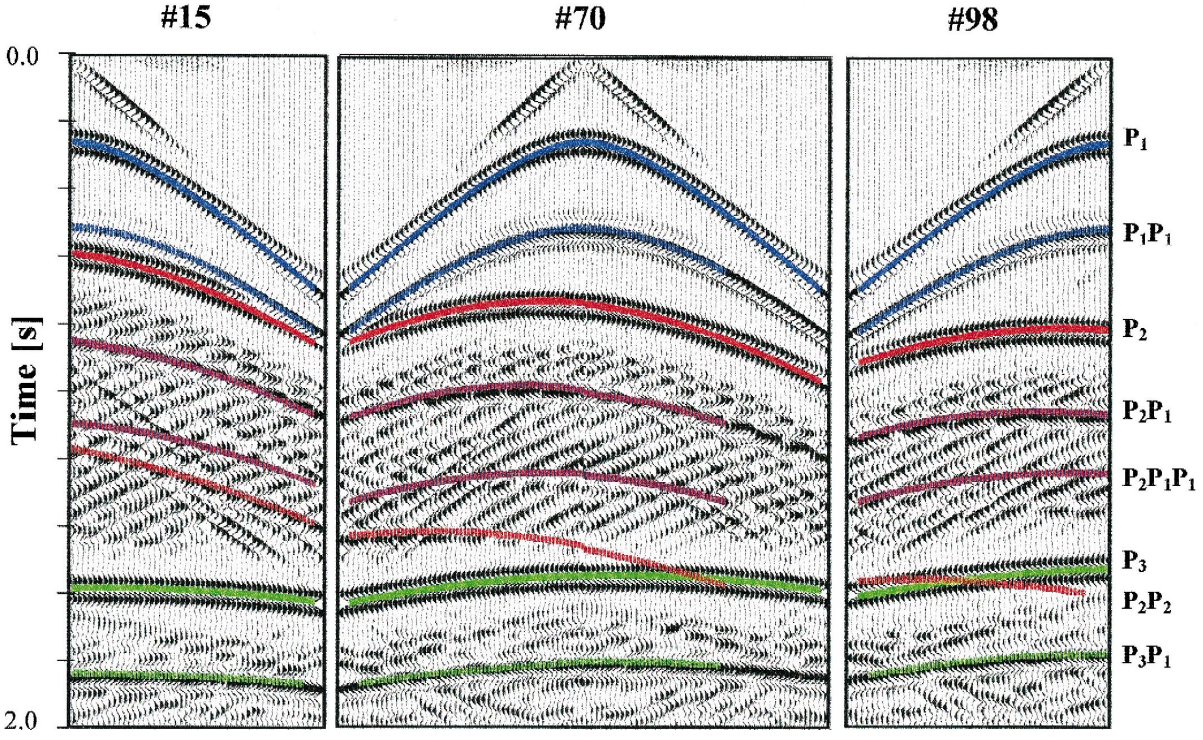

Fig. 9. Predicted multiple travel times in three shot-gathers (#15, #70 and #98). Their location on the seismic line is indicated in Fig. 4. The trace increment is 20 m. AGC has been applied in order to enhance weak multiples. The events are shown in different colors. Labels are according to the multiple ray schemes in Fig. 8. Note: the moveout of the primaries (P_1, P_2 and P_3) has been calculated using the estimated emergence angles β_0 and radii of wavefront curvature R_0 in Eq. (3).

be observed in case of the second interface (see P_2 in Fig. 6a,b).

Using the estimated parameters of the normal ray R_0 and β_0 in Eq. (4) gives the extrapolated angle of emergence of the primary wavefronts from the three interfaces at different offsets. Fig. 7 shows as an example the results for one shot-gather with especially high differences between analytical and estimated wavefront parameters of the normal ray. The extrapolated values essentially coincide with the analytical results. Only for the second reflector the differences at far offsets are higher due to the already mentioned higher differences in β_0 and R_0. Knowing the emergence angles of the primary reflections for all shot–receiver pairs, we can find those primary traces which generate a specified multiple by using the appropriate multiple conditions. The goal in this example is to predict and attenuate four first order and one second order surface related multiple as well as one interbed multiple (Fig. 8).

After the multiple generating primary traces have been determined, the multiple travel times

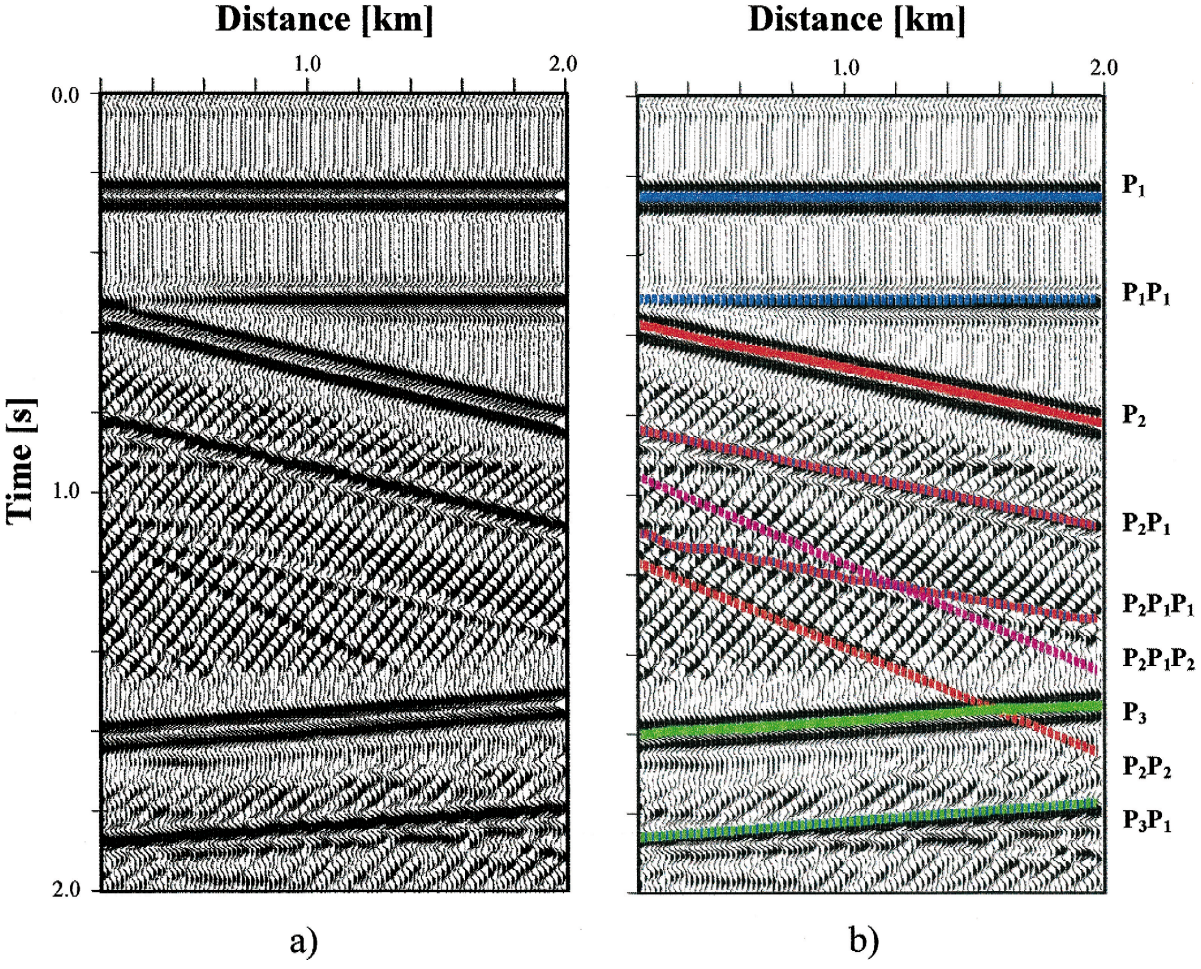

Fig. 10. Minimum offset section before multiple attenuation. (a) Minimum offset section. (b) Minimum offset section including labeling for picked primaries and predicted multiple events. AGC has been applied in order to enhance multiple energy.

are calculated. The predicted travel times are shown in three shot-gathers in Fig. 9, on different locations along the seismic line. A very good fit between the predicted travel times and that calculated by FD modeling can be observed especially for the first order multiples. The predicted times for the second order surface multiple and the interbed multiple look reasonable but cannot be compared easily with the modeled data because of their weak amplitudes, which are not resolvable in the noisy dataset.

The predicted multiple travel times are also shown in the minimum offset section (Fig. 10). We show the minimum offset section after AGC, because here the multiples are not cancelled like it might be during stacking. The agreement with the modeled data is again very good. In this case, also the predicted second order surface multiple ($P_2P_1P_1$) can be seen in the modeled data. The interbed multiple prediction ($P_2P_1P_2$) is kinematically correct but still, it cannot be compared with the modeled dataset, because of its weak amplitude.

The wavefield cut from the original data-set within time windows around the predicted multiple travel times serves as multiple model in the multiple attenuation process. After t^2-stretching of the original data and the multiple model data, the multiple attenuation (filtering) was done in the parabolic τ–p domain. After the inverse τ–p transform, followed by inverse t^2-stretching, we obtain the results of the multiple filtering in the x–t domain, which are shown for five CDP gathers in Fig. 11. All predicted multiples are strongly attenuated. In Fig. 12 a stacked section before and after multiple attenuation is shown. The only difference in the processing scheme between the two sections is our multiple attenu-

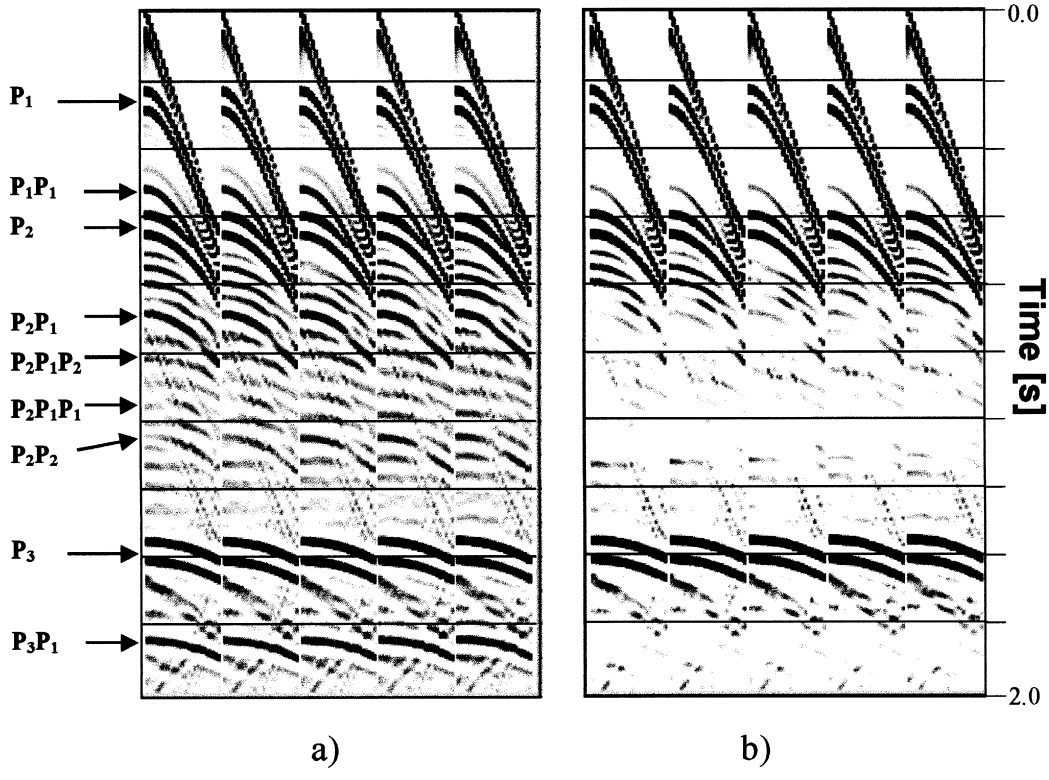

Fig. 11. Results of prediction and subtraction in a collection of five CDP gathers, which are located at about 250 m in Fig. 4. (a) Before multiple attenuation. (b) After multiple attenuation. All multiples are strongly attenuated. Because of noise and very weak amplitudes, the higher order and interbed multiple can hardly be seen in the seismic data.

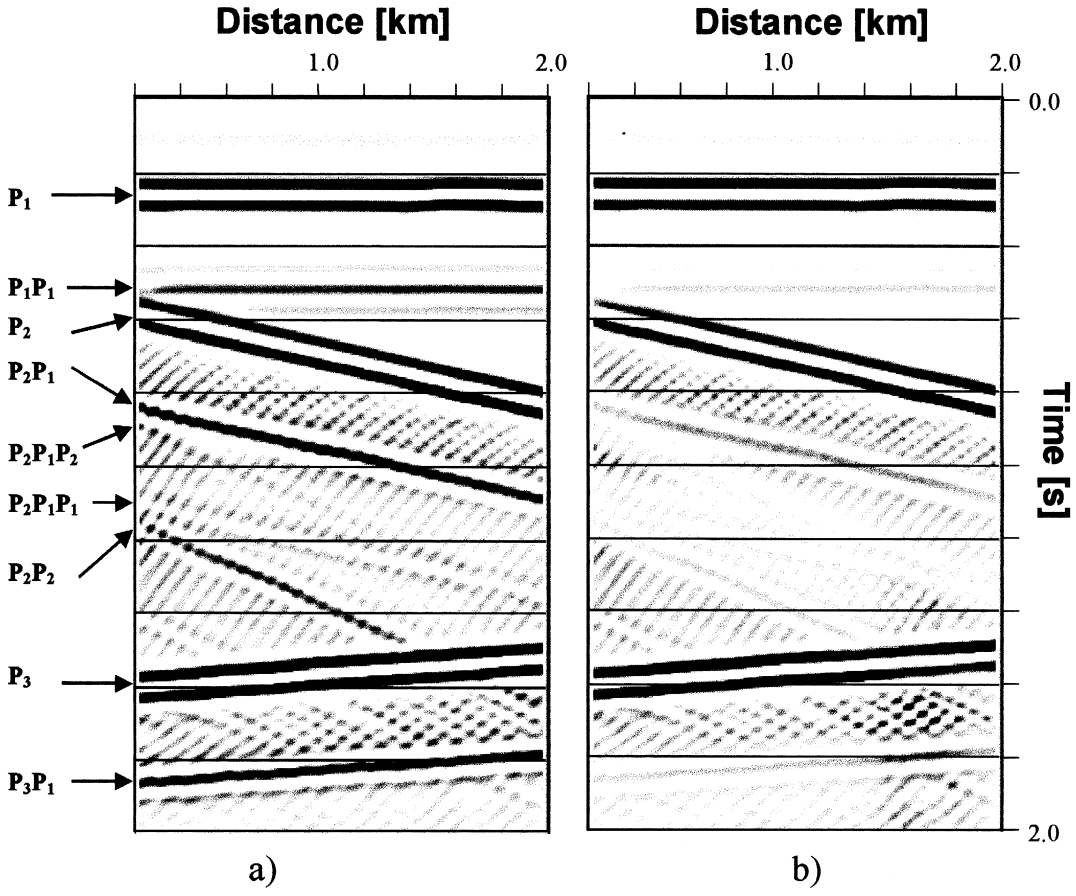

Fig. 12. Stacked section after optimal velocity analysis. (a) Before multiple attenuation. The labels denote the primaries and predicted multiple events. (b) After multiple attenuation. All multiples are well attenuated. Because of noise and very weak amplitudes, the higher order and interbed multiple can hardly be recognized in the seismic data.

ation. Although differential moveout already reduced multiple energy during stacking, the significant improvement due to our multiple attenuation is obvious: all predicted multiples are attenuated and only the primaries and the residual wave-field are left.

5. Conclusions

A new semi-interactive and horizon-based method is proposed for the macro-velocity-independent estimation of kinematic wavefront characteristics, namely emergence angle and radius of wavefront curvature of the normal ray. This procedure is essentially a new implementation of the CSP HI method. A crucial advantage of this approach is that ambiguity problems in cases of different local semblance maxima can be resolved by manual picking of the optimal emergence angles along a horizon. As usual, leading criteria for picking might be smoothness of wavefront parameters along a horizon and a priori information. Additionally, we show a possibility for the use of estimated kinematic wavefront parameters in a multiple prediction and attenuation method, which is valid for surface as well as interbed multiples. Apart from the near surface velocity, it does not need any information on the subsurface model. A repre-

sentative example shows the power of the parameter estimation, prediction and attenuation procedure.

Acknowledgements

We wish to thank the reviewers Dr. Dimitri Lokshtanov, Dr. Martin Karrenbach, Dr. Uwe Kästner and Dr. Robert Essenreiter for their constructive comments as well as BHP Petroleum for supporting this work.

References

Biondi, B., 1992. Velocity estimation by beam stack. Geophysics 57, 1034–1047.

Gelchinsky, B., 1989. Homeomorphic imaging in processing and interpretation of seismic data (fundamentals and schemes). Expanded Abstracts. 59th SEG Meeting, Dallas, 983–988.

Hampson, D., 1986. Inverse velocity stacking for multiple elimination. Journal of Canadian Society of Exploration Geophysics 22, 44–55.

Jakubowicz, H., 1998. Wave equation prediction and removal of interbed multiples. Extended Abstracts. 60th EAGE Meeting, Leipzig, 1–28.

Kelamis, P., Chiburis, E., Shahryar, S., 1990. Radon multiple elimination, a practical methodology for land data. Expanded Abstracts. 60th SEG Meeting, San Francisco, 1611–1613.

Keydar, S., Gelchinsky, B., Berkovitch, A., 1996. Common shot point stacking and imaging method. Journal of Seismic Exploration 5, 261–274.

Keydar, S., Landa, E., Gelchinsky, B., Belfer, I., 1998. Multiple Prediction using the homeomorphic-imaging technique. Geophysical Prospecting 46, 423–440.

Landa, E., Keydar, S., Belfer, I., 1999a. Multiple prediction and attenuation using wavefront characteristics of multiple-generating primaries. Leading Edge 18 (1).

Landa, E., Belfer, I., Keydar, S., 1999b. Multiple attenuation in the parabolic $\tau - P$ domain using wave front characteristics of multiple-generating primaries. Geophysics, in press.

Shultz, P.S., Clearbout, J.F., 1978. Velocity estimation and downward continuation by wavefront synthesis. Geophysics 43, 691–714.

Zhou, B., Greenhalgh, S.A., 1994. Linear and parabolic $\tau - p$ transforms revisited. Geophysics 59, 1133–1149.

Zhou, B., Greenhalgh, S.A., 1996. Multiple suppression by 2D filtering in the parabolic $\tau - p$ domain: a wave-equation-based method. Geophysical Prospecting 44, 375–401.